Calcium Phosphate Phase Identification Using XPS and Time-of-Flight Cluster SIMS

ARTICLE *in* ANALYTICAL CHEMISTRY · JANUARY 1999

Impact Factor: 5.64 · DOI: 10.1021/ac9806963 · Source: PubMed

Anal. Chem. **1999,** *71,* 149−153

Calcium Phosphate Phase Identification Using XPS and Time-of-Flight Cluster SIMS

Charles C. Chusuei and D. Wayne Goodman*

Department of Chemistry, Texas A&M University, P.O. Box 30012, College Station, Texas 77842-3012

Michael J. Van Stipdonk, Dina R. Justes, and Emile A. Schweikert

Center for Chemical Characterization and Analysis, Texas A&M University, College Station, Texas 77843-3144

Reproducible time-of-flight cluster static secondary ion mass spectra (ToF-SSIMS) were obtained for various standard calcium phosphate (CP) powders, which allowed for phase identification. X-ray diffraction was not able to detect signals from microscopic amounts of CP (∼15 mmol m^{-2}). The phases studied were α-tricalcium phosphate [α-$Ca_3(PO_4)_2$], *β*-tricalcium phosphate [*β*-$Ca_3(PO_4)_2$], amorphous calcium phosphate [$Ca_3(PO_4)_2 \cdot xH_2O$], octacalcium phosphate [$Ca_8H_2(PO_4)_6 \cdot H_2O$], brushite ($CaHPO_4 \cdot 2H_2O$), and hydroxyapatite [$Ca_{10}(PO_4)_6(OH)_2$]. The SIMS spectra were obtained via bombardment with $(CsI)Cs^+$ projectiles. X-ray photoelectron spectroscopy (XPS) core levels of the P 2p, Ca 2p, and O 1s orbitals and the relative O 1s loss intensity were examined. The PO_3^-/PO_2^- ratios from ToF-SSIMS spectra in conjunction with XPS of the CP powders showed much promise in differentiating between these phases at microscopic CP coverages on the metal oxide surface.

In the study of biological calcification on metal oxide implants, there is current interest in detecting phase transformations of microscopic biominerals on the surface. Calcium phosphate (CP) materials are important in the study of biomineralization since they are either precursors or major components of bone and teeth. Studies were undertaken in order to develop bioactive CP coatings on implant materials to improve the biocompatibility of biomineral with the implant[1] using the constant composition (CC) method[2,3] to model the nucleation and growth of CP materials on Brunauer−Emmett−Teller (BET) characterized metal oxide surfaces on colloidal seeds. The CP phases of these materials were well identified using X-ray diffraction (XRD). However, it should be noted that the examination of the nucleation and growth of these phases using the CC method did not distinguish between adsorbed material and precipitated material. The formation of the CP phases leading to hydroxyapatite [$Ca_{10}(PO_4)_6(OH)_2$, HAP], the principal component of bone material, was likely controlled largely by precipitation rather than adsorption. Several studies were performed investigating the precursor phase CPs that led to the formation of HAP.[4−12] However, when microscopic amounts of CP were present on the surface, the quantity of material was too low to be detected by conventional XRD methods.[13] Being able to characterize low levels of CP phases at the onset of nucleation and growth on model oxide surfaces is the goal of our study.

In a methodology developed by Nooney et al.[14] to study adsorbed species on the metal oxide surface, a CP solution (composed of 3.5 mM $CaCl_2$ and 119 g mL^{-1} as KH_2PO_4 adjusted to pH 6.5) was adsorbed onto ultrahigh vacuum (UHV)-characterized metal oxide surfaces via solid−liquid adsorption using a peristaltic pump.[15] The surface was rinsed with Millipore CO_2-free H_2O to elute weakly bound ions on the surface and hence remove precipitated material. Coverages as low as ∼5 mmol of P m^{-2} of CP were deposited on hematite (Fe_2O_3), alumina (Al_2O_3), and titania (TiO_2) surfaces, and the kinetics of phosphate adsorption were measured on the surface using temperature-programmed desorption (TPD) and Auger electron spectroscopy (AES). While submonolayer amounts of CP were observed to nucleate and grow on the surface as shown by the resulting TPD and AES uptake curves, the phase of the adsorbing species was not determined in this study because clearly defined CP standards could not be adsorbed onto the surface (via solid−liquid adsorption) for subsequent surface analysis.

Surface-sensitive analysis methods were needed for phase elucidation on such a system. Phase characterization using XPS was attempted in our laboratory, examining the core level shifts,

(1) Song, L.; Campbell, A. A.; Li., X. S.; Bunker, B. C. *Mater. Res. Soc. Symp. Proc.* **1996**, *414*, 35−41.
(2) Sheehan, M. E.; Nancollas, G. H. *J. Invest. Urol.* **1980**, *7*, 446−450.
(3) Ebrahimpour, A.; Zhang, J.; Nancollas, G. H. *J. Cryst. Growth* **1991**, *113*, 83−91.
(4) Brown, W. E. *Clin. Orthoped.* **1966**, *44*, 205−220.
(5) Eanes, E. D.; Termine, J. D.; Nylen, M. U. *Calcif. Tissue Res.* **1973**, *12*, 143−148.
(6) Nancollas, G. H.; Tomazic, B. *J. Phys. Chem.* **1974**, *78*, 2218−2225.
(7) Nancollas, G. H. *J. Cryst. Growth* **1977**, *42*, 185−193.
(8) Boskey, A. L.; Posner, A. S. *J. Phys. Chem.* **1976**, *80*, 40−45.
(9) Cheng, P.-T. *Calcif. Tissue Int.* **1987**, *40*, 339−343.
(10) Eidelman, N.; Chow, L. C.; Brown, W. E. *Calcif. Tissue Int.* **1987**, *41*, 18−26.
(11) Abbona, F.; Baronnet, A. *J. Cryst. Growth* **1996**, *165*, 98−105.
(12) Liu, Y.; Wu, W.; Sethuraman, G.; Nancollas, G. H. *J. Cryst. Growth* **1997**, *174*, 386−392.
(13) Nancollas, G. H.; Zhang, J. In *Hydroxyapatite and Related Materials*; Brown, P. W., Constantz, B., Eds.; CRC Press: Boca Raton, 1994; pp 73−81 and references therein.
(14) Nooney, M. G.; Campbell, A.; Murrell, T. S.; Lin, X.-F.; Hossner, L. R.; Chusuei, C. C.; Goodman, D. W. *Langmuir* **1998**, *14*, 2750−2755.
(15) Murrell, T. S.; Corneille, J. S.; Nooney, M. G.; Vesecky, S. M.; Chusuei, C. C.; Hossner, L. R.; Goodman, D. W., submitted to *Rev. Sci. Instrum.*

10.1021/ac9806963 CCC: $18.00
Published on Web 11/19/1998

but yielded inconclusive results. We thus turn to secondary ion mass spectrometry (SIMS) as a viable surface analysis method.

Qualitative SIMS studies[16,17] using monatomic projectiles on β-tricalcium phosphate (β-TCP) and HAP have been attempted; but, distinguishing between these two phases could not be confidently done due to significant erosion of the surface that accompanied getting adequate S/N for analysis. Since the static limit was already reached (and likely exceeded) in these studies, spectra from the two phases were very similar and difficult to distinguish from one another. For successful analysis, increased secondary ion (SI) yields with decreased surface erosion is needed. Monatomic primary ions produce, in general, low yields of sputtered secondary polyatomic ions. The most abundant negative SIs from phosphate materials are polyatomic entities such as PO_2^- ($m/e = 63$) and PO_3^- ($m/e = 79$). The use of polyatomic primary ions has been shown to improve the SI yield; the most significant improvement is for polyatomic SIs.[18−20] With this in mind we felt that the sensitivity and efficiency for molecular characterization (with reduced surface erosion) of CP material would be improved using time-of-flight static cluster SIMS (ToF-SSIMS) with polyatomic primary ions.

We thus present in this study the utility of polyatomic cluster ToF-SSIMS as a new analytical method for CP phase elucidation. ToF-SSIMS, XRD, and XPS were used to characterize the same CP powder samples for a comparative study. The powders selected were those of interest in the nucleation and growth scheme for HAP as predicted by Ostwald's step rule.[1]

EXPERIMENTAL SECTION

Apparatus. XRD analysis was performed using a Rigaku RU 200 X-ray diffractometer with a Cu $K\alpha_{1,2}$ rotating anode and a graphite crystal monochromator operated at 180 mA, 50 kV, and 9 kW. This same XRD apparatus was unsuccessfully used to analyze the above-mentioned ∼15 mmol of P m^{-2} coverage on the TiO_2 surface. XPS was performed in an ion-pumped Perkin-Elmer PHI 560 system using a PHI 25-270AR double-pass cylindrical mirror analyzer (CMA). A Mg Kα anode operated at 12 kV and 200 W with a photon energy of $h\nu = 1253.6$ eV was used. The base pressure of the XPS instrument after a bakeout was ∼1 × 10^{-10} Torr, and the operating system pressure during the scans was ∼5 × 10^{-9} Torr. The pass energy of the XPS high-resolution scans was 50 eV. The ToF-SSIMS apparatus, described fully elsewhere,[21] used a ^{252}Cf radioactive source to generate $(CsI)_nCs^+$ (n = 0, 1, 2) and C_{60}^+ primary ions. The projectiles were accelerated to 20-keV impact energy. Negative SIs were accelerated to −7 keV and mass analyzed by time-of-flight. Using event-by-event bombardment and detection along with a coincidence-counting protocol,[22] SI mass spectra from multiple projectiles were generated simultaneously (instrument and target surface conditions remained constant through the measurement). The system pressure for the ToF-SSIMS measurements was ∼3 × 10^{-7} Torr or lower.

Reagents. The following powders were obtained from Clarkson Chromatography Products, Inc. (South Williamsport, PA) and used as received: α-tricalcium phosphate [α-$Ca_3(PO_4)_2$, α-TCP], β-tricalcium phosphate [β-$Ca_3(PO_4)_2$, β-TCP], amorphous calcium phosphate [$Ca_3(PO_4)_2 \cdot xH_2O$, ACP], octacalcium phosphate [$Ca_8H_2(PO_4)_6 \cdot 5H_2O$, OCP], brushite ($CaHPO_4 \cdot 2H_2O$, DCPD), and HAP.

Procedure. Each of the powder samples were mounted onto the respective XRD, XPS, and ToF-SSIMS instruments and scanned. In the XRD measurements, the powders were packed into a flat aluminum sample holder. Data were acquired between 5 and 55° in 2θ with a step size of 0.02° and a count time of 10 s per step. The phases of the powders were thus verified prior to the surface-sensitive analytical techniques, XPS and ToF-SSIMS, that followed. In the XPS measurements, the powders were mounted on a 1.0 cm × 1.0 cm × 0.1 mm polycrystalline Ta foil substrate with double-sided tape (3M Scotch). Sputter-cleaned Cu $2p_{3/2}$ (932.7 eV) and Au $4f_{7/2}$ (84.0 eV) core level peaks (from foils) were used to calibrate the spectrometer's binding energy (BE) range.[21] Signal from adventitious carbon as a BE standard at 284.7 ± 0.2 eV was used to correct for charging on the substrate as described by Barr.[23,24] XPS high-resolution scans were performed for the C 1s, Ca $2p_{3/2}$, Ca $2p_{1/2}$, P 2p, and O 1s core levels. In the ToF-SSIMS measurements, double-sided tape was used to mount the powders onto the stainless steel sample holder. At least two sample preparations and three experimental trials were performed for each of the CP powders.

RESULTS AND DISCUSSION

XRD. Spectra of the CP powders were acquired and shown in Figure 1. Diffraction patterns were consistent with those of the respective powders in the literature.[25,26] At macroscopic amounts of material, all of the CP phases can easily be distinguished by using the 2θ peak positions and relative intensities of the peaks with respect to one another as a fingerprint. In a preliminary experimental run in this laboratory, ∼15 mmol of P m^{-2} was adsorbed onto the TiO_2 thin-film (∼50 Å thick) on a polycrystalline Ta substrate. The thin-film preparation, adsorption method, and calibration method used was the same as previously described.[14] XRD analysis was then taken. An XRD spectrum of ∼15 mmol m^{-2} of CP on thin-film TiO_2 is shown (7) for comparison. The background intensity, denoted by the arrows, was due to the aluminum sample holder. Clearly, from spectrum 7, no structural information can be obtained from XRD at these low coverages. No signal from the adsorbed CP molecules was observed in the XRD pattern and hence phase characterization was not available using this analysis method. Thus, other methods were necessary for phase elucidation.

XPS. The core level BE positions and Ca/P of the CP powders are summarized in Table 1. High-resolution XPS scans were curve-

(16) Spoto, G.; Ciliberto, E.; Allen, G. C. *J. Mater. Chem.* **1994**, *4*, 1849−1850.
(17) Allen, G. C.; Cilibert, E.; Fragalà; Spoto, G. *Nucl. Instrum. Methods B* **1996**, *116*, 457−460.
(18) Benguerba, M.; Brunelle, A.; Della-Negra, S.; Depauw, J.; Joret, H.; Le Beyec, Y.; Blain, M. G.; Schweikert, E. A.; Ben Assayag, G.; Sudraud, P. *Nucl. Instrum. Methods B* **1991**, *62*, 8−22.
(19) Van Stipdonk, M. J.; Harris, R. D.; Schweikert, E. A. *Rapid Commun. Mass Spectrom.* **1996**, *10*, 1987−1991.
(20) Harris, R. D.; Van Stipdonk, M. J.; Schweikert, E. A. *Int. J. Mass Spectrom. Ion Processes* **1998**, *174*, 167−177.
(21) Blain, M. G.; Della-Negra, S.; Joret, H.; Le Beyec, Y.; Schweikert, E. A. *J. Vac. Sci. Technol. A* **1990**, *8*, 2265−2268.
(22) Seah, M. P. *Surf. Interface Anal.* **1989**, *14*, 488.
(23) Barr, T. L.; Seal, S. *J. Vac. Sci. Technol. A* **1995**, *13*, 1239−1246.
(24) Barr, T. L. *Modern ESCA*; CRC Press: Boca Raton, 1994; Chapter 6 and references therein.
(25) *JCPDS International Centre for Diffraction Data* (database software), ver. 1.30; Newtown Square, PA, 1997 and references therein.
(26) McIntosh, A. O.; Jablonski, W. L. *Anal. Chem.* **1956**, *28*, 1424−1427.

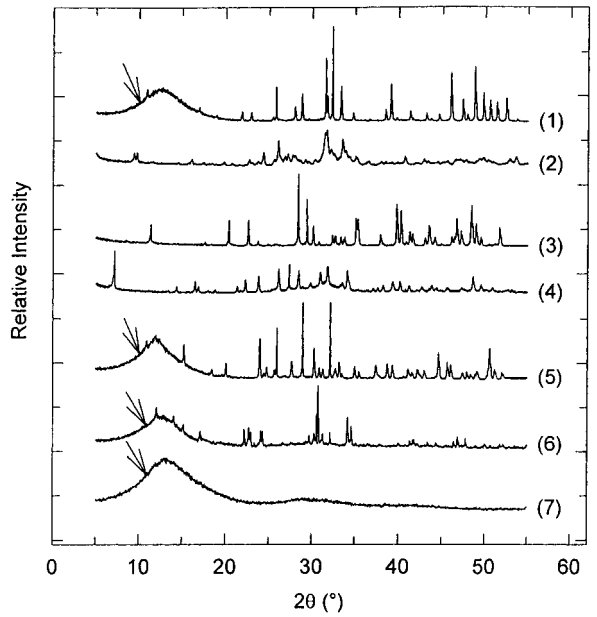

Figure 1. XRD spectra of calcium phosphate powders: (1) HAP, (2) OCP, (3) DCPD, (4) ACP, (5) β-TCP, and (6) α-TCP. Spectrum 7 is that of ~15 mmol m^{-2} CP adsorbed onto titania from solution. Background intensity seen at $2\theta \approx 7-17°$ is an experimental artifact from the aluminum sample holder.

Table 1. XPS Core Levels of CP Phases

phase	P 2p (eV)	Ca $2p_{1/2}$ (eV)	Ca $2p_{3/2}$ (eV)	O 1s (eV)	Ca/P ratio[a]
α-TCP	133.3	350.7	347.2	531.0	1.20 (1.50)
β-TCP	133.1	350.6	347.0	530.9	1.40 (1.50)
HAP	133.5	350.7	347.2	531.1	1.59 (1.67)
ACP	133.1	350.6	347.1	531.1	1.13 (1.50)
OCP	133.2	350.7	347.1	531.0	1.20 (1.33)
DCPD	133.6	350.8	347.3	531.6	0.74 (1.00)

[a] The experimentally measured Ca/P ratios are shown with their respective theoretical ratios in parentheses.

fitted, and the peak area intensities of the core levels were normalized to their respective atomic sensitivity factors.[27] The mole fractions of the powders were obtained from intensities of the P 2p and Ca $2p_{3/2}$ core levels. The precision of the BE measurements are ±0.2 eV and the peak full width at half-maximums (fwhm) of the core levels are ~2.5 eV. The measured XPS core levels were in good agreement with BEs of the same CP powders studied previously using biased referencing.[28]

In principle, it should be possible to distinguish between the various CP phases by measurements of the mole fractions of Ca and P from XPS. In practice, however, the measured Ca/P in these runs were all consistently lower than the theoretical Ca/P. It was found that prolonged exposure of the CP powders to the X-ray source (1 h) resulted in even lower Ca/P values. Thus, some X-ray-induced decomposition of the Ca substituent in the powders most likely occurred. The amount of deviation from the theoretical value was indicative of the stability of the CP phases. All of the CP powders, with the exception of HAP, was reported to be relatively unstable and capable of transforming into the other phases after prolonged exposure to air.[29] HAP, the most stable of the CP phases (in air) was the least affected by the photodegradation, having a 4.8% error. HAP had the highest Ca/P, which is consistent with the expected ratio. ACP and DCPD were the most unstable of the phases and had the greatest deviation from the theoretical values, 24.6 and 26.0%, respectively. Even with the largest error (26%), DCPD can be distinguished from the other phases based on the Ca/P mole fraction. However, it was more difficult to distinguish α-TCP, β-TCP, OCP, ACP, and HAP from each other. The shifts of the Ca $2p_{1/2}$ and Ca $2p_{3/2}$ core levels gave no differentiation between the phases given the ±0.2 eV uncertainty. Similarly, in examining the XPS core level shifts the O 1s core level of the DCPD was clearly different from the other phases being at least +0.5 eV higher in BE than for the other phases (e.g., ACP and HAP). DCPD proportionately had the largest amount of hydrate groups (H_2O) with respect to the PO_4^{3-} groups in the molecular makeup than the other phases. The higher BE of the O 1s (532.6 eV) was closer to that reported for H_2O (533.0 eV).[30] The O 1s and P 2p core levels can be used in conjunction for phase identification. For example, a P 2p BE of 133.4−133.7 eV accompanied by a 531.0−531.2 eV O 1s BE was diagnostic of HAP. Similarly, a P 2p level of 133.4−133.7 eV with an O 1s level of 531.5−531.7 eV signified DCPD on the surface.

Since the CP phases under consideration had O atoms from different functional groups (namely phosphate O and hydroxyl O), Lu et al.[31] suggested that these CP phases may be sensitive to variations in XPS loss intensity of the O 1s core level with respect to the main peak. XPS loss signals have been used as a way to extract chemical information regarding different functional organic groups (e.g., C−O, C═O, C−O−H, etc.) by looking at the loss peaks resulting from plasmons from the C 1s core level.[25] Similarly, loss peaks from the O 1s core level may be used to elucidate different O-containing environments that were present in the CP phases, such as P═O and O−H. Figure 2 shows an XP spectrum of DCPD indicating the loss and core level intensities from the O 1s orbital with curve-fitted lines. The percent loss intensity was calculated by dividing the loss peak area by the core level peak area. In our XPS measurements, the measured O 1s XPS loss intensities had peak centers at 554.8 and 568.4 eV with fwhm of ~7.9 and ~6.6 eV, respectively. Comparison of the area of the 568.4 eV loss intensity with that the of the core level was attempted as was done previously.[31] In comparing these peak area ratios there were very little, if any, differences between the relative loss intensities between the CP phases. All of the relative loss values were between ~6 and 8%. CP differentiation with our data improved when both loss peak areas were used. The percent loss taken from the sum of the areas underneath both peaks (normalized to the O 1s core level intensity) of the CP phases as well as the differing proportions of O functional group environments are listed in Table 2. Differentiation was possible between α-TCP and β-TCP from the XPS O 1s loss intensity where only PO_4^{3-} groups were present. The standard deviations (STDs) of the α-TCP and

(27) Wagner, C. D.; Riggs, W. M.; Davis, L. E.; Moulder, J. F. *Handbook of X-ray Photoelectron Spectroscopy*; Muilenberg, G. E., Ed.; Perkin-Elmer Corp.: Eden Praire, MN, 1979; p 188.
(28) Landis, W. J.; Martin, J. R. *J. Vac. Sci. Technol. A* **1984**, *2*, 1108−1111.
(29) Clarkson Chromatography Products, Inc. South Williamsport, PA 17701.
(30) Wagner, C. D.; Zatko, D. A.; Raymond, R. H. *Anal. Chem.* **1980**, *52*, 1445−1451.
(31) Lu, H.; Campbell, C. T.; Ratner, B. D. Characterization of Apatite and Related Calcium Phosphate Surfaces by XPS. 24th Annual Meeting of the Society for Biomaterials, San Diego, CA, April 23−25, 1998; Paper 35.

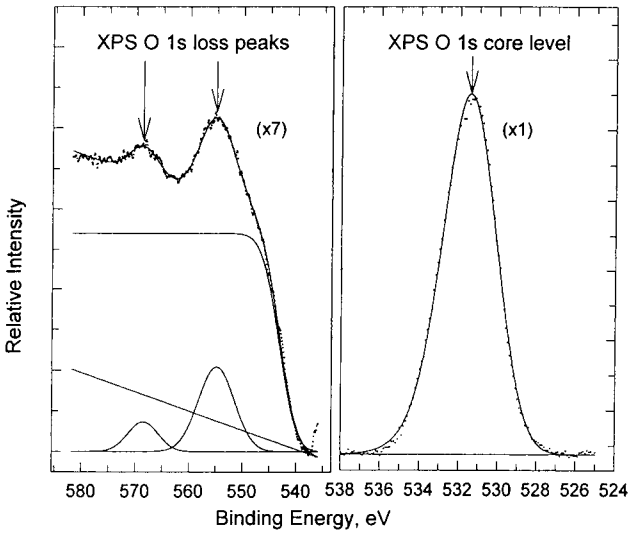

Figure 2. XPS intensity from the O 1s core level showing curve-fitted Gaussian line shapes. The subtracted background for the O 1s loss peaks at 554.8 and 568.4 (±0.2) eV is a linear combination of linear and cumulative function backgrounds.

Table 2. XPS Loss Intensity of O 1s from CP Phases

phase	% loss[a]	O-containing groups
α-TCP	20.0 ± 0.5	PO_4^{3-} groups only
β-TCP	24 ± 2	PO_4^{3-} groups only
HAP	17 ± 3	3 PO_4^{3-} groups to 1 OH^- group
ACP	24 ± 3	2 PO_4^{3-} groups to *x* H_2O groups
OCP	20 ± 4	6 PO_4^{3-} groups to 5 H_2O groups
DCPD	12 ± 3	1 PO_4^{3-} group to 2 H_2O groups

[a] The percentage loss intensity was relative to the main O 1s core level peak at 100%.

β-TCP measurements were relatively small. There were apparently differences in the electronic environments between the two crystal structures of α-TCP (monoclinic) and β-TCP (rhombahedral). In addition, HAP can be distinguished from β-TCP and ACP, but not with α-TCP, OCP, or DCPD. Of all of the CP phases, DCPD seemed to have the lowest percent loss intensity. This finding was in agreement with results of Lu et al. on common CP phases analyzed,[31] which were more precise. We attribute the enhanced precision to the superior transmission characteristics of the hemispherical analyzer used in their experiments compared to the double-pass CMA used in ours. DCPD had the highest hydroxyl O to phosphate O ratio, which corresponded to a low percent loss compared to the other CP phases in our measurements. Otherwise, no obvious trend with the different oxygen environments to the percent loss was observed. However, it should be noted that in our preliminary experiments of adsorbing CP material via solid−liquid adsorption onto a TiO_2 surface, 80% of the O 1s signal came from the oxide overlayer, thus limiting the utility of the XPS loss analysis method.[32]

ToF-SSIMS. Secondary electrons emitted from the sample surface were used to count the number of incident primary ions in the SIMS analysis. Therefore, only negative SI spectra were recorded. This fact did not hamper the analysis of the CP substrates as PO_3^- ($m/e = 79$) and PO_2^- ($m/e = 63$) are intense

(32) Chusuei, C. C.; Goodman, D. W., unpublished results.

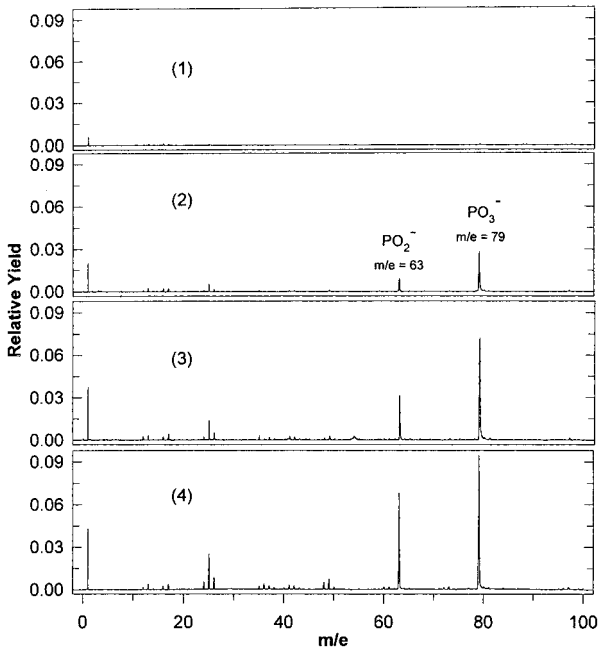

Figure 3. SI mass spectra produced polyatomic ToF cluster ions: (1) $(CsI)_2Cs^+$, (2) $(CsI)Cs^+$, (3) Cs^+, and (4) C_{60}^+. These mass spectra were acquired simultaneously. Masses at $m/e = 63$ and 79 were indicative of the PO_2^- and PO_3^- species, respectively.

SI peaks representative of all phosphate-containing materials. Previous studies have determined that polyatomic primary ions were more efficient for generating substrate-specific SIs from inorganic targets than atomic primary ions. Polyatomic ions of increasing size and complexity, however, were also more prone to generate reduction reactions during SI formation.[33,34] Figure 3 shows negative ToF-SSIMS spectra using Cs, $(CsI)Cs$, $(CsI)_2Cs$, and C_{60} primary ions on a CP sample prepared from a solution containing $CaH_4(PO_4)_2 \cdot H_2O$. The raw data divided by the number of CsI projectiles generated is shown in the figure. The solution had been applied to the SIMS instrument target and allowed to dry. Since the CP was deposited from aqueous solution, the purity of the phase could not be guaranteed due to possible phase transformation.[35] The spectra in Figure 3 display the relative yield (the number of secondary ions detected per incident primary ion) versus secondary ion mass. Each spectrum was acquired from the same sample target with a primary ion dose, for each projectile, of not more than 10^7 ions cm^{-2}. The $(CsI)Cs^+$ proved to be the optimum projectile for these experiments, producing the highest yield of PO_3^- with the minimum projectile induced reduction to PO_2^-. Similar results have recently been reported using (CsI)-Cs^+ projectiles on other inorganic targets.[36,37] Figure 4 shows the

(33) Van Stipdonk, M. J.; Harris, R. D.; Schweikert, E. A. *Rapid Commun. Mass Spectrom.* **1997**, *11*, 1794−1798.

(34) English, R. D.; Van Stipdonk, M. J.; Harris, R. D.; Schweikert, E. A. In *Proceedings of the 11th International Conference on Secondary Ion Mass Spectrometry*, Orlando, FL, September 7−12, 1997; Gillen, G., Lareau, R., Bennett, J., Stevie, F., Eds.; J. Wiley and Sons, Ltd.: Chichester; 1997; pp 589−592.

(35) Abbona, F.; Baronnet, A. *J. Cryst. Growth* **1996**, *165*, 98−105.

(36) Van Stipdonk, M. J.; Santiago, V.; Schweikert, E. A. In *Proceedings of the 46th ASMS Conference on Mass Spectrometry and Allied Topics*, Orlando, FL, May 31−June 4, 1998, p 1224.

(37) Van Stipdonk, M. J.; Justes, D. R.; Santiago, V.; Schweikert, E. A. *Rapid Commun. Mass Spectrom.*, in press.

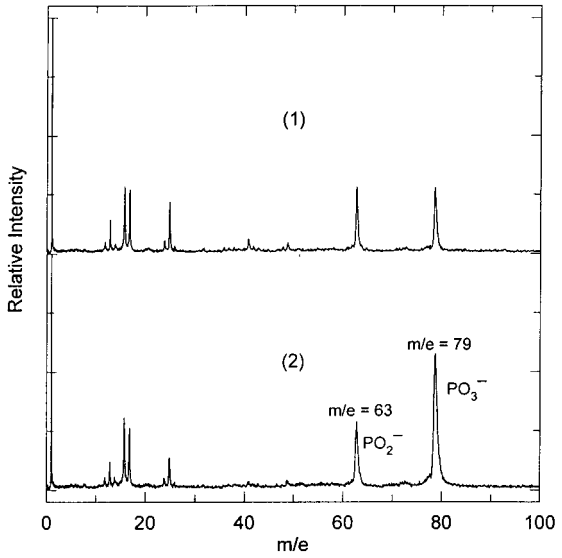

Figure 4. SI mass spectra using $(CsI)Cs^+$ polyatomic ToF cluster ions: (1) OCP and (2) DCPD.

negative SI mass spectra of DCPD and OCP, which are qualitatively representative of all the CP powders. The SI intensity in each spectrum was normalized to the number of incident primary ions and is shown relative to the most abundant SI in this figure. In addition, small mass peaks corresponding to H^-, O^-, and OH^- were present. Higher mass SI such as polyatomic ions containing PO_2^- and PO_3^- units were not observed at the $(CsI)Cs^+$ ion dose used in the experiments. It should be noted that with the dose of Cs^+ projectiles used (less than 10^7 ions cm^{-2}), no phosphate peaks were observed in the SI mass spectra. Though PO_2^- and PO_3^- can be observed at higher doses with Cs^+, differences in the relative PO_3^-/PO_2^- SI yields between CP phases were ambiguous. The spectra produced by Cs^+ projectiles (not shown) were instead dominated by low-mass ions such as H^-, O^-, and OH^-. We observed during initial experiments that different phosphate materials produced different relative yields of PO_3^- and PO_2^-.

The relative intensities of these two SIs were examined for sensitivity to the various CP phases using $(CsI)Cs^+$ projectiles. The results of this study are summarized in Table 3. Similar to the XPS analysis, DCPD gave distinct results from the other CP phases. Unambiguous identification of the CP phases were readily available from the relative SI yields from PO_2^- and PO_3^- for β-TCP, OCP, and ACP; such differentiation was not possible with XPS. ACP could be distinguished from β-TCP and OCP, which was not distinguishable with either the XPS core levels or relative O 1s loss signals. However, given the standard deviations, α-TCP and HAP were indistinguishable from one another. A decrease in the mass resolution due to the higher surface roughness of the HAP powder (compared with the other CP phases) resulted in a relatively larger standard deviation in the SI yield compared with α-TCP. Grinding of the HAP powder into finer particulates did not improve the STD.

Table 3. Relative PO_3^-/PO_2^- SI Ratios from Various CP Powders

β-TCP	0.701 ± 0.009	OCP	1.08 ± 0.03
HAP	0.84 ± 0.03	ACP	1.38 ± 0.05
α-TCP	0.85 ± 0.02	DCPD	2.6 ± 0.1

In summary, ToF-SSIMS when used in conjunction with XPS core levels and loss peaks showed promise in being able to elucidate CP phase as a function of growth at small coverages that was not amenable to XRD. The ToF-SSIMS signals were substantial ($S/N \geq 10$) at the $\sim$15 mmol m^{-2} CP coverage; XRD at these coverages exhibited no signal. Experiments are currently in progress utilizing these two surface-sensitive techniques to elucidate CP phase change involved in the adsorption of these biologically relevant minerals on metal oxide surfaces.

ACKNOWLEDGMENT

We thank Dr. Allison A. Campbell at the Pacific Northwest National Laboratory (PNNL) for many helpful discussions regarding this project. PNNL is operated for the U.S. Department of Energy by Battelle Memorial Institute under Contract DE-AC06-76RL0. We also thank Prof. Charles T. Campbell for providing us with XPS and SIMS spectral data related to our study before publishing their paper. C.C.C. thanks the Associated Western Universites, Inc. and PNNL for support. This work was also funded by NSF Grant CHE-9727474.

Received for review June 30, 1998. Accepted October 16, 1998.

AC9806963